VOLUME 113, NUMBER 1
JANUARY 2, 1991

JOURNAL
OF THE
AMERICAN
CHEMICAL
SOCIETY

SHAPES Empirical Force Field: New Treatment of Angular Potentials and Its Application to Square-Planar Transition-Metal Complexes

Viloya S. Allured, Christine M. Kelly, and Clark R. Landis*

Contribution from the Department of Chemistry and Biochemistry, University of Colorado, Boulder, Boulder, Colorado 80309-0215. *Received March 19, 1990*

Abstract: The application of empirical force field methods to transition-metal complexes is limited by the difficulty of describing complex molecular shapes with valence force field methods and by the lack of tested empirical parameters. The SHAPES force field is a new treatment of angular distortion (three body) terms that is based on angular overlap considerations. Angular potential energies are expressed as periodic Fourier terms in spherical internal coordinates. This formulation provides a general description of many idealized geometries including the trigonal-bipyramid, square-plane, octahedron, square-pyramid, and other geometries. Three approaches to the parametrization of the SHAPES force field (normal coordinate analysis, ab initio calculation, and structure-based optimization) are presented and are shown to give similar results. Application of the SHAPES force field to a variety of square-planar rhodium complexes demonstrates that empirical force field methods can be used to estimate the structures of these complexes with impressive accuracy (bond length rmsd = ±0.02 Å, bond angle rmsd = ±3°).

I. Introduction

Computer-aided molecular design requires the implementation of computational procedures for the prediction of molecular structures and energetics. A variety of computational techniques, ranging from ab initio to semiempirical to completely empirical techniques, can be employed in the estimation of molecular structures and energetics.[1] Because of their computational efficiency and accuracy, empirical force field (EFF) methods frequently are the methods of choice, particularly for large molecules in their ground states. Over the last 15 years, developments and refinements of the EFF techniques (e.g. MM2,[2] CHARMM,[3] AMBER,[4] etc.) have provided organic and biochemical researchers with powerful computational tools. In contrast, efforts directed at the development of more general EFF's capable of describing the varied structures of inorganic compounds have been sparse.

This is not to say that EFF methods have not been successfully applied to inorganic problems. A partial listing of reported applications of EFF calculations to transition-metal complexes includes conformational analysis of chelate rings,[5] analysis of Franck–Condon factors in electron-transfer reactions,[6] modeling of cavity sizes in macrocycle chelation,[7] structural analyses of metal–metal multiple bonds,[8] and the simulation of ligand arrangements in metal clusters.[9] Although these applications provide firm evidence for the feasibility of applying EFF methods to transition-metal complexes, current force field formulations

* Address correspondence to this author at the Department of Chemistry, University of Wisconsin, Madison, WI 53706.

(1) Fruhbeis, H.; Klein, R.; Wallmeier, H. *Angew. Chem., Int. Ed. Engl.* **1987**, *26*, 403.
(2) Allinger, N. L.; Yuh, Y. H.; Lii, J.-H. *J. Am. Chem. Soc.* **1989**, *111*, 8551.
(3) Brooks, R.; Bruccoleri, R. E.; Olafson, B. D.; States, D. J.; Swaminathan, S.; Karplus, M. *J. Comput. Chem.* **1983**, *4*, 187.
(4) (a) Weiner, P. K.; Kollman, P. A. *J. Comput. Chem.* **1981**, *2*, 287. (b) Weiner, S. J.; Kollman, P. A.; Case, D. A.; Singh, U. C.; Ghio, C.; Alagona, G.; Profeta, S.; Weiner, P. *J. Am. Chem. Soc.* **1984**, *53*, 1.
(5) Brubaker, G. R.; Johnson, D. W. *Coord. Chem. Rev.* **1984**, *53*, 1.
(6) (a) Bond, A. M.; Hambley, T. W.; Snow, M. R. *Inorg. Chem.* **1985**, *24*, 1920. (b) Endicott, J. F.; Brubaker, G. R.; Ramasami, T.; Kummar, K.; Dwarakanath, K.; Cassel, J.; Johnson, D. *Inorg. Chem.* **1983**, *22*, 3754.
(7) (a) Thom, N. J.; Fox, C. C.; Boeyens, J. C. A.; Hancock, R. D. *J. Am. Chem. Soc.* **1984**, *106*, 5947. (b) Drew, M. G. B.; Rice, D. A.; Silong, S.; Yates, P. C. *J. Chem. Soc., Dalton Trans.* **1986**, 1081.
(8) Boeyens, J. C. A. *Inorg. Chem.* **1985**, *24*, 4149–4152.
(9) Lauher, J. W. *J. Am. Chem. Soc.* **1986**, *108*, 1521–1531.

0002-7863/91/1513-1$02.50/0

are not generalized readily to the varieties of molecular shapes exhibited by many inorganic (both main group and transition metal) complexes.

Factors limiting the application of EFF methods to transition-metal complexes can be divided into (1) limitations inherent in the generalized valence force fields and (2) difficulties in parametrization of the force field. In this paper, we first address the former issue and outline our development of a new force field, SHAPES, which obviates some of these limitations. The remainder of this paper describes the development of force field parameters for square-planar transition-metal complexes.

II. Empirical Force Field Formulations

1. General Considerations. Most molecular mechanics routines are based on valence force field models.[2-4] The simple valence force fields express the total potential energy as the sum of bond-stretching, angle-bending, out-of-plane-bending (or improper dihedrals), torsional (or dihedral), and nonbonded terms (eq 1).

$$E = E_{\text{bond stretch}} + E_{\text{angle bend}} + E_{\text{torsions}} + E_{\text{improper torsions}} + E_{\text{nonbonded}} \quad (1)$$

Bond stretch (eq 2) and angle bending (eq 3) terms are typically expressed by harmonic potentials derived from a truncated Taylor expansion of the potential energy in internal coordinates. Torsional distortions are characterized by periodic behavior and large amplitudes that cannot be described well by harmonic potentials; consequently, Fourier series trucated at one, two, or three terms are commonly used (eq 4). Improper terms (eq 5) are required to represent out-of-plane distortion potentials accurately (e.g. out-of-plane distortion at a trigonal planar center) and to prevent racemization about chiral, tetrahedral centers. Nonbonded terms comprise van der Waals, hydrogen bonding, and electrostatic interactions. Commonly, Lennard-Jones (6-12 or 6-10) or Buckingham formulas are used for the van der Waals interactions. Electrostatic interactions most frequently are modeled by atom-based point charge potentials. By normal convention, the calculation of nonbonded terms is not performed for atoms connected through one or two bonds (1,2 and 1,3 interactions) because these contributions are assumed to be implicit in the bond-stretch and bond-bend force constants.[10] These simple force fields may be improved by the addition of off-diagonal terms (e.g. stretch-bend), but at the cost of additional parameters.

$$E_{\text{bond stretch}} = k_r(r - r_0)^2 \quad (2)$$

(r = bond length, r_0 = equilibrium bond length, k_r = force constant)

$$E_{\text{angle bend}} = k_\Theta(\Theta - \Theta_0)^2 \quad (3)$$

(Θ = bond angle, Θ_0 = equilibrium bond angle, k_Θ = force constant)

$$E_{\text{torsion}} = \sum_i k_{\Phi_i}[1 + \cos(n_i\Phi + \delta)] \quad (4)$$

(Φ = torsion angle, n_i = periodicity, k_{Φ_i} = barrier height/2, δ = phase shift)

$$E_{\text{improper}} = k_\lambda(\lambda - \lambda_0)^2 \quad (5)$$

(λ = improper angle, λ_0 = equilibrium improper angle, k_λ =force constant)

The application of simple valence force field computations to coordination compounds, although possible as demonstrated by the examples mentioned previously, is problematic. The first type of problem is revealed by the large variation of ligand-metal-ligand (L-M-L) bond angles observed at transition-metal centers. For example, four-coordinate metal complexes having d^8 configuration (e.g. Rh(I), Ir(I), Pd(II), and Pt(II) complexes) exhibit a strong preference for square-planar geometries. On the basis of an idealized square-planar geometry, L-M-L angles of 90° (cis ligands) and 180° (trans ligands) are expected. Indeed, many experimental structures conforming well to this idealized geometry have been found.[11] However, when four bulky ligands such as trimethylphosphine are coordinated to a single rhodium(I) center,[12] large distortions toward a tetrahedron are observed, resulting in transoid bond angles of 150°. Such large distortions (30° from the equilibrium position) suggest a soft angular deformation potential. A harmonic angular deformation potential is not likely to describe adequately the deformation energetics for such large amplitude motions. One possible solution to this problem is the addition of higher order terms to the harmonic expression, albeit at the cost of additional parametrization.

A related problem involving the use of a harmonic angular deformation potential concerns the behavior of the function at the angular limit (e.g. $\theta_{\text{L-M-L}} = 180°$ for a bent triatomic such as water). At this limit, harmonic functions have cusps whereas the slope of $E(\theta)$ should be zero. This behavior underscores the intrinsic anharmonicity of the angular deformation potential, particularly in the region of large distortions that are not uncommon for transition-metal complexes. (It should be noted that harmonic bond-stretching terms, also, do not reach proper limiting values upon bond rupture. Thus, Morse potentials and related functions provide better descriptions of $E(r)$.[13] However, bond-stretching potentials are much steeper than angular deformation potentials and equilibrium geometries commonly have bond lengths that lie within the harmonic region.)

A third problem encountered in the application of simple valence force fields to inorganic complexes is the definition of unique angles and corresponding equilibrium values. We refer to this as the *unique labeling problem.* For example, *cis*-diaminodichloroplatinum(II) requires two N-Pt-Cl equilibrium angle values (90° and 180°). The unique labeling problem arises for any molecular shape with the possibility of cis and trans ligand orientations (this includes T-shaped, square-planar, trigonal-bipyramidal, square-pyramidal, and octahedral idealized geometries). On this basis, description of the frequently observed trigonal-bipyramidal and square-pyramidal geometries, in particular, requires cumbersome treatment due to the existence of three different L-M-L equilibrium angle values. Since cis and trans orientations are not possible for tetrahedral, trigonal-planar, and linear geometries, the problem of defining unique angles and equilibrium values is not an issue for organic structures. Incorporation of multiple equilibrium positions and redundant atom labeling schemes permits simple valence force fields to circumvent these problems but requires tedious over-definition of the molecular topology.

Empirical force field simulations of transition-metal-complex geometries may be complicated by the presence of strong electronic effects, also. We include variable coordination numbers and formal oxidation states as well as the trans influence in these effects. For organic systems, the different molecular geometries brought about by changes in hybridization about a central carbon atom are treated by the development of parameters specific for different bonding situations. By analogy, the variation of metal geometries brought about by changes in formal oxidation state and coordination numbers, in principle, can be accommodated by the development of parameters specific for various oxidation states and coordination numbers. The trans influence, although not unique to transition-metal complexes, can result in particularly large changes in metal-ligand bond lengths. For example, Pt-Cl bond lengths systematically vary from 2.28 to 2.44 Å in a series of mononuclear, four-coordinate Pt(II) complexes as the electronegativity of the trans ligand is varied.[14]

(10) Allinger, N. L.; Burkert, U. *Molecular Mechanics*; American Chemical Society: Washington, 1982.

(11) A search of four coordinate rhodium complex structures on the Cambridge Structure Database reveals an average cis L-M-L bond angle of 89° and an average trans L-M-L bond angle of 175°.

(12) Jones, R. A.; Real, F. M.; Wilkinson, G.; Galas, A. M. R.; Hursthouse, M. B.; Malik, K. M. A. *J. Chem. Soc., Dalton Trans.* **1980**, 511.

(13) Murrell, J. N.; Carter, S.; Farantos, S. C.; Huxley, P.; Varandas, A. J. C. *Molecular Potential Energy Functions*: Wiley and Sons: Chichester, 1984.

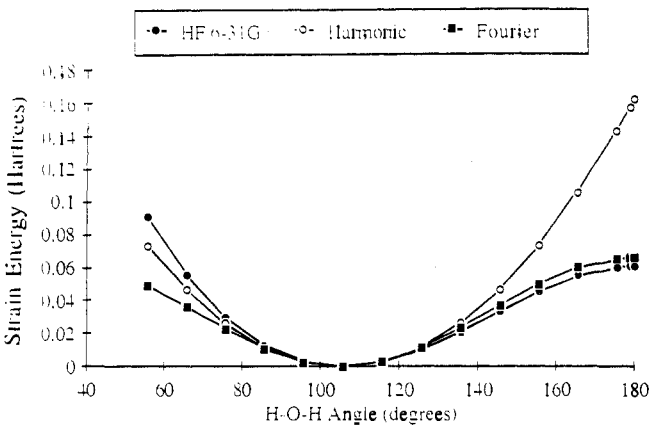

Figure 1. Comparison of potential energy surfaces for angular distortion of water calculated by (●) the restricted Hartree-Fock method with a 6-31G* basis set, (○) a harmonic force field (k = 0.191 hartree/rad^2, θ_0 = 105.5°), and (■) a Fourier term (k^F = 0.0652 hartree, n = 2.42, ψ = 74.5°).

The problems discussed above point out limitations in the ability of harmonic angular potentials to describe the complex and easily distorted shapes of inorganic complexes. (Other limitations in the application of empirical force fields to organometallic clusters have been discussed by Lauher.[9]) To overcome some of these limitations of the simple valence force fields we have developed a new treatment of angular potential energy terms based on the premise that angular potentials should reflect changes in central atom–ligand orbital overlaps. The resulting force field, referred to as the SHAPES force field, differs from valence force fields in that periodic Fourier terms are used for angular potentials within a spherical internal coordinate system description.

2. Fourier Angular Potentials. Harmonic angular potential energy terms have the unwanted properties of overestimating bond angle distortion energies at bond angles far from the equilibrium position and of being cusped at bond angles of 180°. A softer form of the angular potential is used in SHAPES: a single Fourier term in the bond angle (eq 6). Here ϕ represents the bond angle,

$$E_{EFF} = k^F[1 + \cos(n\phi + \psi)] \quad (6)$$

n is the periodicity of the cosine function, ψ is the phase shift which determines the positions of the minima, and k^F is the "force constant" which determines the steepness of the function about the minima.

Figure 1 illustrates angular potential energy curves for water calculated by an ab initio method and by empirical methods using harmonic and Fourier terms with parameters derived from the ab initio calculation. In this figure the periodicity and the phase of the Fourier term have been adjusted so that the minimum occurs at the 104° equilibrium bond angle (ϕ_0) and a maximum occurs at the linear geometry with use of relationships 7 and 8. The Fourier force constant, k^F, is interconverted with the harmonic

$$n = \frac{\pi}{\pi - n\phi_0} \quad (7)$$

$$\psi = \pi - n\phi_0 \quad (8)$$

force constant, k^H, using relationship 9. From the figure it is seen

$$k^F = 2k^H/n^2 \quad (9)$$

clearly that the Fourier term is a superior representation of the distortion potentials at large bond angles, closely tracking the ab initio potential and reaching a maximum at 180°. Therefore, Fourier terms (and the related cosine expansions) are better behaved functions for angular distortion potentials than the harmonic terms, in part because the Fourier term simulates the effect of changes in orbital angular overlaps (see Appendix 1). Also note that both empirical calculation methods underestimate the potential energies at small bond angles, underscoring the need for

(14) Hartley, F. R. *Chem. Soc. Rev.* **1973**, *2*, 163.

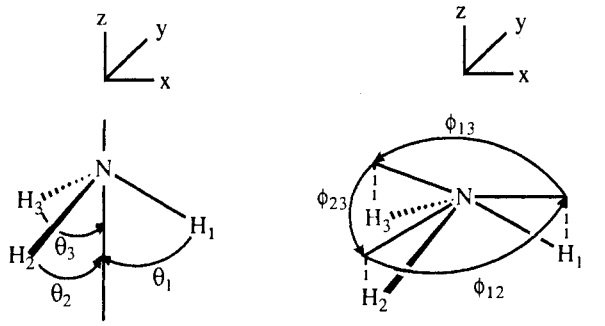

Figure 2. Coordinates used to describe angular deformations in the ammonia molecule. The ϕ angles are made by the N–H bond vectors with the axis defined as normal to the plane of the hydrogen nuclei and containing the nitrogen nucleus. The θ angles are defined by the angles made by the *projections* of the N–H bond vectors into the plane which is normal to the reference axis and contains the nitrogen nucleus. The lengths of the N–H bonds are defined as R_{N-H} whereas the lengths of their projections are defined as r_{N-H}.

appropriately scaled 1,3-interaction terms in the force field (such terms are not included in the SHAPES force field or in other popular force fields).

3. Spherical Internal Coordinates. The description of complex molecular geometries (e.g. those having multiple equilibrium angle values) with standard internal coordinates is troublesome. Such geometries are described more readily by using internal coordinates based on a spherical coordinate system (spherical internal coordinates).

Definition of a molecular coordinate system based on spherical internal coordinates requires a reference axis. In the SHAPES formulation, this reference axis always contains the central atom, which is the origin of the local coordinate system. For trigonal-planar, trigonal-pyramidal, and square-planar geometries the reference axis is defined as the line normal to the plane of the ligands and passing through the central atom. For the example of ammonia illustrated in Figure 2, the reference axis is colinear with the z axis. For molecular geometries having an axial ligand, i.e. trigonal-bipyramidal, square-pyramidal, octahedral, and monovacant octahedral idealized geometries, the reference axis is defined as colinear with the line connecting the central atom to a single ligand identified by the user as axial. Having defined a reference axis two angles (θ and ϕ) and a bond length (radial vector) uniquely define all nuclear positions. The θ angles are simply the angles made by the central atom-to-ligand bond vectors with the reference axis. The ϕ angles are defined by the angles made by the projections of the central atom-to-ligand bond vectors into the plane normal to the reference axis (this will be referred to as the ϕ plane) that contains the central atom (i.e. the x–y plane in the treatment of ammonia).

As shown previously for water, expression of angular deformation potentials with a single Fourier term yields a superior description because the function is equivalent to a harmonic function for small distortions, softer than harmonic functions at large distortions, and behaves properly (maximizes) at the angular limit of 180°. Thus, Fourier terms in ϕ and θ are employed in the SHAPES force field. *The periodicities of the Fourier terms in ϕ and θ are determined by the symmetries of the idealized geometries.* Thus, the trigonal-pyramidal geometry of ammonia is viewed as having 3-fold periodicity in θ and a periodicity in ϕ that is adjusted to give a maximum at the planar structure and a minimum at the experimental structure. The potential energy terms for ammonia as a function of spherical internal coordinates are given below.

$$E = \sum_{\theta} k_\theta[1 + \cos(n\theta + \psi_\theta)] + \sum_{\phi} \mathrm{wt}\, k_\phi[1 + \cos(n\phi + \psi_\phi)] \quad (10)$$

where

$$\mathrm{wt} = \left(\frac{r_{ML}r_{ML'}}{R_{ML}R_{ML'}}\right)^2 \quad (11)$$

and

$$R_{ML} = \text{the M–L bond length} \quad (12)$$

and

$$r_{ML} = \text{the length of the M–L vector projected into the } \phi \text{ plane} \quad (13)$$

Note that the ϕ Fourier terms are multiplied by a weighting term, wt. This weighting is required to properly scale down the contributions to the θ energy terms as one or both of the ligands moves out of the plane in which ϕ is defined (the ϕ term becomes zero for axial ligands). For ammonia, the effect of this weighting term is to give full weight to the energy and forces along ϕ in the trigonal-planar geometry but less weight to these terms in the trigonal-pyramidal geometry. In a trigonal bipyramid small movements of an axial ligand away from the reference axis could lead to large variations in $E(\phi)$ if weighting were not included. Such a weighting scheme can be rationalized by using angular overlap considerations (Appendix 2).

A contour plot of the angular potentials for ammonia with use of a 3-fold periodicity ($n = 3$, $\psi = 180°$) for the ϕ distortion (corresponding to minima at $\phi = 0°$, 120°, and 240°) and $n = 5.1$ (and $\psi = 98.9°$) for the θ distortion term (to give minima at $\theta = 54.7°$ and 125.3°) is shown in Figure 3. This contour diagram shows the expected minima at $\theta = 120°$ and $\phi = 54.7°$ and 123.5° and a maximum at $\phi = 90°$ along the inversion trajectory. Note also the presence of a minimum at $\theta = 0°$ corresponding to "fusion" of the H ligands. An inherent drawback of the periodic functions is the presence of a minimum at $\theta = 0°$; in principle this false minimum could be removed either by expansion of the Fourier term or by inclusion of appropriate 1,3-interaction terms as discussed for water. The current force field utilizes neither since reasonable starting geometries are not directed to these "false" minima and the form of the 1,3 potential is not obvious.

For simple idealized geometries such as trigonal-pyramidal or trigonal-planar structures, the SHAPES force field offers few advantages over valence force fields with improper dihedrals other than softer deformation potentials and an improved description of inversion modes. However, for descriptions of complicated geometries (e.g. trigonal bipyramidal) the periodicity of the Fourier terms and the spherical internal coordinate formulation can be used to considerable advantage. In the SHAPES force field, a trigonal-bipyramidal structure is readily formulated with 3-fold periodicity in the ϕ terms and 4-fold periodicity in the θ terms (corresponding to minima at 120° intervals in ϕ and 90° intervals in θ). Similarly, a square-planar structure is formulated with 4-fold periodicity in ϕ and 2-fold periodicity in θ. This formulation is readily extended to virtually any idealized geometry (see Table I). SHAPES has the advantage of matching natural periodicities (i.e. proper axes of symmetry) in angular potentials for idealized geometries resulting in, we think, an intuitive description of molecular geometries. Because of the periodic nature of the force field, SHAPES does not require separate parameters for cis and trans ligand arrangements, thus avoiding the cumbersome "unique labeling" problem. In comparison with common valence force fields, SHAPES replaces the harmonic bond angle and improper dihedral terms with adjustable periodic functions in ϕ and θ. In rather crude analogy with simple bonding arguments, the trigonometric ϕ and θ terms simulate the effects of variations in orbital overlaps on molecular stabilization.

4. Implementation of the SHAPES Force Field. We have integrated FOURIER and SHAPES as options in the CHARMM program originally developed by Karplus and co-workers.[3] CHARMM was selected for the computational superstructure because of the powerful combination of minimization (particularly the adopted basis set Newton–Raphson minimization), molecular dynamics, parameter optimization, and data analysis routines.

The FOURIER option causes angular deformation terms to be calculated with Fourier expression 6 in bond angles (not spherical internal coordinates). Use of Fourier terms is invoked in the CHARMM residue topology file (RTF). Parameters for the Fourier terms are stored in the FOURIER section of the parameter input file. If the required parameters are not found in the FOURIER section of the parameter file the parameters are derived from the corresponding harmonic terms using (eqs 7–9). These calculations lead to a potential that maximizes at $\theta = 180°$ but is identical with the harmonic function at angle values close to θ_0.

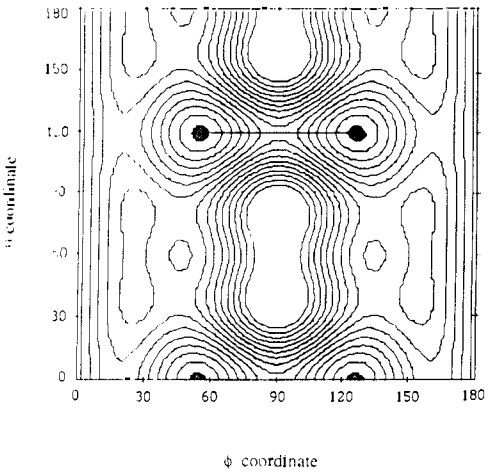

Figure 3. Contour plots for angular deformations of ammonia calculated according to the SHAPES empirical force field formulation. The shaded areas indicate minima and the solid, horizontal lines indicate the inversion trajectory. Potential energies are expressed as arbitrary units.

The SHAPES option (i.e. utilization of Fourier terms of appropriate periodicities within a spherical internal coordinate system) is invoked via the keyword SHAPE in the CHARMM RTF. This keyword is followed by the name of the central atom, the name of the axial atom, and the name of the shape type (see Table I). Appropriate parameters must be included in the parameter file. There is no separate SHAPES block; the angle values of all periodicities required for a particular shape are taken from the FOURIER block of the parameter file. The subroutine SHAPES is called once for each central atom to be treated by using the SHAPES force field in the internal energy calculation subroutines. First, necessary values such as the number of ligands and the parameters and coordinates for this shape are loaded into local arrays. Coordinates are transformed to a local coordinate system with the central atom at the origin and the specified axial ligand along the z axis. It should be noted that the calculated energy depends slightly (<1 kcal in most cases) on which atom is identified as axial for trigonal-bipyramidal, square-pyramidal, and octahedral geometries. A subsequent version of SHAPES will correct this limitation. If the structure is trigonal pyramidal, trigonal planar, or square planar, the reference axis is found by subroutine AXIAL, which calculates the axis normal to the best plane of ligand atoms that passes through the central atom. Calculation of the entire local coordinate system takes place on each call of the SHAPES subroutines during a minimization or dynamics trajectory. Thus, the local coordinate system changes as the molecular geometry changes.

For each ligand, the θ angle is determined and the corresponding energies (eq 10) and analytical first derivatives with respect to θ are calculated. The energy is added to the angular strain energies and the first derivatives are converted to derivatives in the local Cartesian coordinate system by using the chain rule. Next, ϕ angles are calculated as are the energies (eq 10) and the first derivatives with respect to ϕ and with respect to local Cartesian coordinates. These calculations include the weighting formula (eqs 10 and 11). As a final step, the Cartesian derivative vectors for all the atoms are rotated back to the global molecular coordinates and added to the main Cartesian derivative arrays. The energy terms, which are scalar, do not require rotation. Analytical first derivatives, only, for the SHAPES terms are currently supported. A subsequent version of the program will include analytical second derivatives.

Normally we use the SHAPES force field for transition-metal-centered bond angles only; all other bond angles are treated

Table I. Treatment of Idealized Geometries in SHAPES

geometry	keyword	reference axis	angular terms
trigonal pyramidal	PYR	normal to ligand plane	3-fold periodicity in ϕ adjusted periodicity in θ
trigonal planar	PYR	normal to ligand plane	3-fold periodicity in ϕ adjusted phase and periodicity in θ
square planar	PLAN	normal to ligand plane	4-fold periodicity in ϕ 2-fold periodicity in θ
tetrahedral	none	none	adjusted Fourier in bond angles
trigonal bipyramidal	TRIG	user-specified ligand	3-fold periodicity in ϕ 4-fold periodicity in θ
square pyramidal	SQUA	user-specified ligand	4-fold periodicity in ϕ adjusted periodicity in θ
octahedral	OCTA	user-specified ligand	4-fold periodicity in ϕ 4-fold periodicity in θ

with the harmonic or Fourier approximation. For highly strained systems the softer Fourier-based terms are expected to give lower values of the strain energy. For example, force field calculations on cyclopropane with the standard CHARMM parameters lead to similar geometries with use of either Fourier or harmonic angular terms. However, the angular strain energies differ by 18 kcal/mol (78.62 kcal/mol for the harmonic expression vs 60.2 kcal/mol for the Fourier expression).

III. Application of the SHAPES Force Field: Square-Planar Transition-Metal Complexes

The SHAPES force field contains a treatment of angular terms that can be readily extended to a variety of molecular geometries. A second goal of this work is the parametrization of the SHAPES force field to aid in the study and design of selective homogeneous catalysts. The remainder of this paper focuses on square-planar, d^8 complexes of Rh(I), Ni(II), Pd(II), and Pt(II). These late-transition-metal complexes act as intermediates in a variety of homogeneous, metal-catalyzed transformations including hydrogenation,[15] hydroformylation,[16] hydrocyanation,[17] hydrosilation,[18] and isomerization[19] reactions. We are particularly interested in a detailed examination of the structural origins of enantioselectivity for the asymmetric hydrogenation of prochiral olefins catalyzed by chiral Rh(I) complexes.[20]

1. Atom-Labeling Scheme. Metal-containing systems have special considerations not found in simple organic complexes. Some of these prompted the development of the SHAPES force field: large deviations from equilibrium bond lengths and angles for metal complexes, a variety of geometric shapes, and the unique labeling problem. Two other important considerations are the oxidation state of the metal and the trans influence. Therefore, in conjunction with the development of the SHAPES force field, we have developed an atom-labeling scheme that classifies metal atoms by oxidation state and coordination number and classifies ligand atoms according to the nature of the trans ligand.

The SHAPES atom labels consist of a four-field entry, each of which serves to identify the unique environment of that atom. This scheme is summarized in Table II. The metal-atom labels shown in Table II allow expansion to a wide variety of metal coordination modes. For atoms (ligands) connected to metal centers, the trans influence requires adjustment of equilibrium bond length parameters according to the nature of the trans ligand. Our approach is to develop different parameters, hence requiring different atom labels, for different trans arrangements of ligands. However, this approach is not very general and requires extensive parametrization. Our future efforts will use these trans influenced parameters in devising an algorithm for the automatic adjustment of metal–ligand bond lengths based on the partial charge of the trans ligand and the trans bond angle.

Table II. Atom-Labeling Scheme Used in SHAPES

	field	definition
metals	1 and 2	the atom symbol
	3	the oxidation state
	4	the coordination number
ligands	1	the atom symbol (the second field can be used)
	2	an "M" in this or the 3rd field indicates the ligand is bound to a metal
	3	gives the trans ligand (the fourth field can be used)

RH14—four-coordinate rhodium in the +1 formal oxidation state
PMET—phosphorus bound to a metal and trans to a coordinated C=C
PMO—phosphorus bound to a metal and trans to an oxygen
PMP—phosphorus bound to a metal and trans to a phosphorus
ETRH—an olefinic carbon (ethylene) coordinated to Rh
C6R—CHARMM aromatic carbon
CT—CHARMM aliphatic carbon
O—CHARMM carbonyl oxygen

Treatment of π-coordination of unsaturated organics (coordinated ethylene in these examples) presents some difficulties. Our model considers the metal to be attached to the centroid of the unsaturated system (a dummy atom with the label, DETL), rather than directly to the atoms themselves. This model avoids formation of a three-membered, metallocyclopropane ring and the inherently strong interdependence of bond lengths and bond angles within a metallocyclopropane. In addition, the description of the geometry about the metal is simplified by having a single point of attachment of the metal to the unsaturated ligand.

2. Parametrization of Square-Planar Complexes. The development of EFF parameters for transition-metal complexes is complicated by the low frequencies of many metal–ligand vibrational modes,[21] which may be extensively mixed with ligand-based vibrational modes, and by the presence of strong electronic influences (e.g. the trans influence). This first complication affects predominantly the derivation of force constants. The trans influence complicates predominantly the extraction of equilibrium bond lengths. In order to determine the optimum method of parametrization, particularly the determination of force constants about metal centers, we have explored parametrization based on (1) approximate normal coordinate analysis of vibrational spectra, (2) ab initio calculation of force constants, and (3) derivation of force constants and geometric parameters from crystallographic data. The relevant results of these methods will be summarized, only, in the subsequent sections. Further details are available as supplementary material.

2.1. Normal Coordinate Analysis of Square-Planar Metal Complexes. For simple metal complexes approximate normal coordinate analyses can be used to extract estimations of met-

(15) James, B. R. *Homogeneous Hydrogenation*; Wiley: New York, 1974.
(16) Yagupski, G.; Brown, C. K.; Wilkinson, G. *J. Chem. Soc. A* **1970**, 1392.
(17) Tolman, C. A.; McKinney, R. J.; Siedel, W. C.; Druliner, J. D.; Stevens, W. R. *Adv. Catal.* **1985**, *33*, 1.
(18) Speier, J. L. *Adv. Organomet. Chem.* **1978**, *17*, 407.
(19) Tani, K.; Yamagata, T.; Otsuka, S.; Akutagawa, S.; Kumobayashi, H. *J. Chem. Soc., Chem. Commun.* **1982**, 600.
(20) Harada, K. In *Asymmetric Synthesis*; Morrison, J. D., Ed.; Academic: New York, 1985; Vol. 5, Chapter 10.
(21) Nakamoto, K. *Infrared and Raman Spectra of Inorganic and Coordination Compounds*, 3rd ed.; Wiley: New York, 1978.

al–ligand force constants for some of the modes. These modes include metal–ligand stretching force constants, some metal–ligand bending modes, and many of the bending and stretching modes of the coordinated ligand itself. We have used the vibrational analysis facility within CHARMM to perform vibrational simulations on several square-planar complexes using the simple valence force field within CHARMM.

The following complexes[22-41] were considered for vibrational analysis: $[PtCl_4]^{2-}$, $[PdCl_4]^{2-}$, $[Pt(NH_3)_4]^{2+}$, $[Pd(NH_3)_4]^{2+}$, *trans*-$Pt(NH_3)_2Cl_2$, *trans*-$Pd(NH_3)_2Cl_2$, $[Pd(PMe_3)Cl_3]^-$, $[Pt(PMe_3)Cl_3]^-$, *trans*-$^{104}Pd(PEt_3)_2Cl_2$ and *trans*-$^{110}Pd(PEt_3)_2Cl_2$, $[Pt(C_2H_4)Cl_3]^-$ and $[Pt(C_2D_4)Cl_3]^-$, $[Rh(C_2H_4)_2Cl]_2$, and *trans*-$Rh(PMe_3)_2(CO)Cl$ (vibrational analyses are available as supplementary material). These square-planar complexes were chosen because of their relevance to intermediates in reactions catalyzed by late-transition-metal complexes and because most of the vibrational assignments from the literature appear to be well justified.[21]

Given the simplicity of the force field, the observed and calculated vibrational frequencies generally are in good agreement (rmsd $\sim$ 25 cm^{-1}). Most metal–ligand bond stretching resonances are readily identified and do not show extensive mixing (potential energy distributions give $\geq$80% contribution from the stretching mode) with the exception of the phosphine ligands. The modes assigned to metal–phosphine stretching motions are mixed with the C–P–C bending modes; this decreases the certainty of the corresponding force constant determinations. Metal–ligand bending modes occur at frequencies less than 200 cm^{-1}. For these modes the data are too sparse for detailed analysis. For example, it is not possible to differentiate in-plane and out-of-plane modes on the basis of the available data.

Despite these limitations, the normal coordinate analyses demonstrate useful trends in the force constant values. First, free (i.e. not bound to a metal) ligand force constants are compared with those for coordinated ligands. Coordination of a ligand to a transition metal generally lowers the force constants for the ligand-based modes. For example, the N–H stretching force constant lowers from ca. 460 to ca. 410 kcal/(mol·Å^2) for coordinated ammonia. Coordination of ethylene lowers the C–C stretching force constant from 690 to ca. 580 kcal/(mol·Å^2). Similar lowering is seen for the H–N–H bending force constant (from 44 to 40 kcal/rad^2).

Force constants for bending and stretching at the metal center (Table III) are lower than those typically observed for organic compounds, in keeping with the characterization of metal-centered potentials as soft. Thus, metal–ligand stretching force constants for Pt–X vibrations are approximately one-half of the C–X value (e.g. k_{C-Cl} = 260 kcal/(mol·Å^2) vs k_{Pt-Cl} = 100–130 kcal/(mol·Å^2); k_{C-N} = 390 kcal/(mol·Å^2) vs k_{Pt-N} = 160–170 kcal/(mol·Å^2)).

Table III. Comparison of Empirical and ab Initio Force Constants[a]

complex	mode	empirical[a]	ab initio
$Pd(NH_3)_2Cl_2$	Pd–N	130.0[b]	130.12
	Pd–Cl	91.0[b]	95.16
	out-of-plane		
	Pd–N	*d*	57.03
	Pd–Cl	*d*	25.17
	in-plane		
	N–Pd–N	35.0[b]	46.62
	Cl–Pd–Cl	57.0[b]	30.24
	N–Pd–Cl	45.0[b]	44.97
$Pt(NH_3)_2Cl_2$	Pt–N	170.0[b]	192.8
	Pt–Cl	115.0[b]	125.8
	out-of-plane		
	Pt–N	*d*	48.67
	Pt–Cl	*d*	25.21
	in-plane		
	N–Pt–N	60.0[b]	120.67
	Cl–Pt–Cl	75.0[b]	49.07
	N–Pt–Cl	60.0[b]	83.28
$[Rh(PH_3)_4]^+$	Rh–P	90.0[c]	54.25
	Rh–P (out-of-plane)	26[c]	20.46
	P–Rh–P (in-plane)	38[c]	43.09

[a] Bond stretch force constant units: kcal/(mol·Å^2); angle bend force constant units: kcal/(mol·rad^2). [b] Obtained from normal coordinate analysis of vibrational data (supplementary material). [c] Obtained from structure-based parametrization of force constants for P–Rh–P (section III.2.3). [d] Normal coordinate analysis does not distinguish between the out-of-plane and the in-plane motions.

Bending force constants for X–M–X bond angles average about 0.4 of the M–X stretching force constant value (e.g. k_{N-Pt-N}/k_{Pt-N} = 0.36; $k_{Cl-Pt-Cl}/k_{Pt-Cl}$ = 0.46). Stretching and bending force constants for Pd and Rh complexes are approximately 25% less than those for Pt.

Metal–chloride bond stretch force constants vary with the nature of the trans ligand. For the monosubstituted complexes $Pt(C_2H_4)Cl_3^-$ and $Pt(PMe_3)Cl_3^-$ the mutually trans chloride ligands have Pt–Cl force constants of 130 kcal/(mol·Å^2) whereas the chloride ligands trans to C_2H_4 and PMe_3 have Pt–Cl force constants of 127 and 110 kcal/(mol·Å^2), respectively. This trend, which is based on limited data, runs parallel to the trans influence on Pt–Cl bond lengths. In general, the ability of a force field to reproduce metal–ligand bond lengths is not strongly influenced by the values of the bond-stretching force constants. Thus, the trans influence on bond-stretching force constants will not significantly influence structural simulations (but it will influence vibrational simulations). Therefore, our parametrization of *force constants* does not include trans influences.

Empirical force field methods assume that force constants obtained from normal coordinate analysis of one compound can be transferred to other related compounds. Although the trans influence introduces some systematic error in the transfer of metal–ligand stretching force constants, the observed ranges of stretching and bending force constants suggest that transfer of force constants is reasonable. For example, the ranges of measured values for k_{Pt-Cl}, k_{Pt-N}, $k_{Cl-Pt-Cl}$, and k_{N-Pt-N} are 110–130 kcal/(mol·Å^2), 160–170 kcal/(mol·Å^2), 52–75 kcal/(mol·rad^2), and 60–61 kcal/(mol·rad^2), respectively. Clearly, more data are required to test the assumption of transferability of parameters. The structural results presented in subsequent sections provide additional support for the assumption of transferability.

2.2. Ab Initio Estimation of Force Constants. Ab initio and semiempirical calculations of equilibrium geometries and force constants provide alternative methods of empirical parameter development. Particularly for organic compounds, Hartree–Fock calculations have been shown to yield accurate molecular geometries and force constants. Due to the increasing availability of fast computers, ab initio computational methods are practical for the estimation of molecular properties.[42] However, ab initio calculations at metal centers are not without problems. First, a

(22) Crayston, J. A.; Davidson, G. *Spectrochim. Acta* **1987**, *43A*, 559.
(23) Bigorgne, M. *J. Organomet. Chem.* **1978**, *160*, 345.
(24) Howard, J.; Robson, K.; Waddington, T. C. *Spectrochim. Acta* **1982**, *38A*, 903.
(25) Grogan, M. J.; Nakamoto, K. *J. Am. Chem. Soc.* **1966**, *88*, 5454.
(26) Adams, D. M.; Chandler, P. J. *J. Chem. Soc. A* **1969**, 588.
(27) Jesse, B. E.; Meester, M. A. M.; Stephens, D. J.; Vrieze, K. *Inorg. Chim. Acta* **1978**, *26*, 129.
(28) Hiraishi, J.: Shimanouchi, T. *Spectrochim. Acta* **1966**, *22A*, 1483.
(29) Hendra, P. J. *Spectrochim. Acta* **1967**, *23A*, 2871.
(30) Hendra, P. J. *Spectrochim. Acta* **1967**, *23A*, 1275.
(31) Hendra, P. J.; Sadosivan, N. *Spectrochim. Acta* **1965**, *21*, 1271.
(32) Schmidt, K. H.; Müller, A. *Coord. Chem. Rev.* **1976**, *19*, 41.
(33) Perry, C. H.; Athens, D. P.; Young, E. F.; Durig, J. R.; Mitchell, B. R. *Spectrochim. Acta* **1967**, *23A*, 1137.
(34) Schmidt, K. H.; Müller, A. *Inorg. Chem.* **1975**, *14*, 2183.
(35) Hiraishi, J.; Nakagawa, I.; Shimanouchi, T. *Spectrochim. Acta* **1968**, *24A*, 819.
(36) Durig, J. R.; Cox, A. W. *J. Chem. Phys.* **1975**, *63*, 2303.
(37) Durig, J. R.; Hizer, T. J. *J. Raman Spectrosc.* **1986**, *17*, 97.
(38) Durig, J. R.; Chatterjee, K. K. *J. Mol. Struct.* **1982**, *81*, 167.
(39) Duddell, D. A.; Goggin, P. L.; Goodfellow, R. J.; Norton, M. G.; Smith, J. G. *J. Chem. Soc. A* **1970**, 545.
(40) Shobatake, K.; Nakamoto, K. *J. Am. Chem. Soc.* **1970**, *92*, 3332.
(41) Browning, J.; Goggin, P. L.; Goodfellow, R. J.; Norton, M. G.; Smith, J. G. *J. Chem. Soc. A* **1970**, 545.
(42) Hehre, W. J.; Radom, L.; Schleyer, P. v. R.; Pople, J. A. *Ab Initio Molecular Orbital Theory*; Wiley: New York.

suitable basis set must be found that gives accurate results at a reasonable computational cost. We have employed effective core potential (ecp) basis sets[43] in conjunction with both the MESA computational package developed at Los Alamos National Laboratories[44] and the Gaussian88[45] suite of programs. Second, the effectiveness with which these computational methods reproduce molecular properties must be established.

The compounds for which ab initio force constant evaluations have been carried out are *trans*-$Pt(NH_3)_2Cl_2$, *trans*-$Pt(PH_3)_2Cl_2$, *trans*-$Pd(NH_3)_2Cl_2$, *trans*-$Pd(PH_3)_2Cl_2$, and $[Rh(PH_3)_4]^+$. The Pt and Pd complexes were chosen because of the availability of extensive vibrational and structural information for comparison with the ab initio results. The calculations on the Rh complex are more relevant to our immediate parametrization goals and are used to help guide the parametrization of Rh complexes. For each complex, full geometry optimizations were performed followed by single-point molecular energy calculations at small distortions along specific distortion coordinates. Approximate force constants were calculated by fitting the energies along the various distortion coordinates to harmonic potentials in the spherical internal coordinates r, ϕ, and θ.

Optimized geometries for the test complexes adopt a square-planar geometry with ϕ bond angles of 90° ± 2° (cis) and 180° ± 2° (trans) and θ angles of 90° ± 1°. Computed and experimental metal–ligand bond lengths agree for M–N distances only. For M–P and M–Cl bonds, the calculated lengths are greater than experimental lengths by more than 0.10 Å in all of the complexes for all four of the different effective core potential basis sets employed (available as supplementary material). For our examination of equilibrium geometries the ecp1 basis set provides the best combination of efficiency and accuracy.

The inability of Hartree–Fock calculations with use of the ecp basis sets to reproduce equilibrium metal–ligand bond lengths of third row atoms (i.e. the absolute position of the potential well minimum) does not necessarily preclude the calculation of force constants (i.e. the curvature of the potential well). In fact, the force constants that we calculate (Table III) agree quite well with those derived by other means. For $Pt(NH_3)_2Cl_2$ and $Pd(NH_3)_2Cl_2$ complexes, the metal–ligand bond-stretching force constant values average just slightly larger than those derived from normal coordinate analysis (by ca. 7%). The bending force constants show greater individual variation, but the average values are quite similar (62.5 (calc) vs 55 (expt)). Much of the variation in individual values can be attributed to the inability of the normal coordinate analysis of vibrational data to distinguish individual force constants for the interdependent N–Pt–N, Cl–Pt–N, and Cl–Pt–Cl angles. Furthermore the computed force constants reproduce the trend observed from the normal coordinate analyses: force constants for Pt complexes are greater than those for Pd complexes by approximately 25%.

Because the estimation of force constants from ab initio calculations seems to give similar results to most empirical methods, we have extended these estimations to the Rh complex, $[Rh(PH_3)_4]^+$, a complex for which experimental data cannot be obtained readily. Thus, incorporation of ab initio computations into force field parametrization is particularly advantageous for metal complexes.

2.3. Structure-Based Parametrization of Square-Planar Complexes. Equilibrium geometry parameters (r_0 and θ_0) for empirical force fields typically are determined by adjusting the equilibrium parameter values until the best fit between calculated and experimental structures is found. In principle, force constants, also, may be determined by an iterative fitting of computed structures to experimental structures if (1) the calculated structures are sensitive to the force constant values and (2) the experimental structures exhibit significant variation in the geometric features sensitive to the force constant value. For example, P–M–P bond angles show considerable variation and are sensitive to the bending force constant values. In contrast, calculated bond lengths are quite sensitive to the equilibrium bond parameter but rather insensitive to the stretching force constant.

To develop empirical force field parameters (r_0, θ_0, and force constants) we have optimized initial values using a modification of the nonlinear least-squares fitting (OPTI) utility in CHARMM to give the best fit between calculated and observed bond lengths

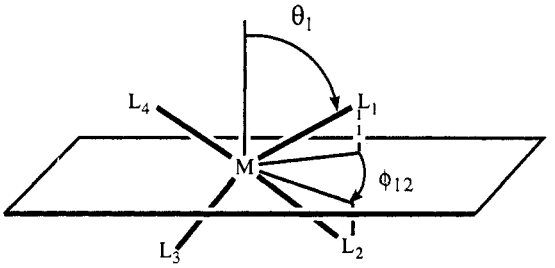

Figure 4. Definition of spherical internal coordinates for square-planar complexes. The θ angles are defined as the angles made by the M–L bond vectors with the reference axis. The reference axis is defined as normal to the best-fit plane of the ligand nuclei and as containing the metal nucleus. The ϕ angles are defined by the angles made by the *projections* of the M–L bond vectors into the plane that is normal to the reference axis and contains the metal nucleus.

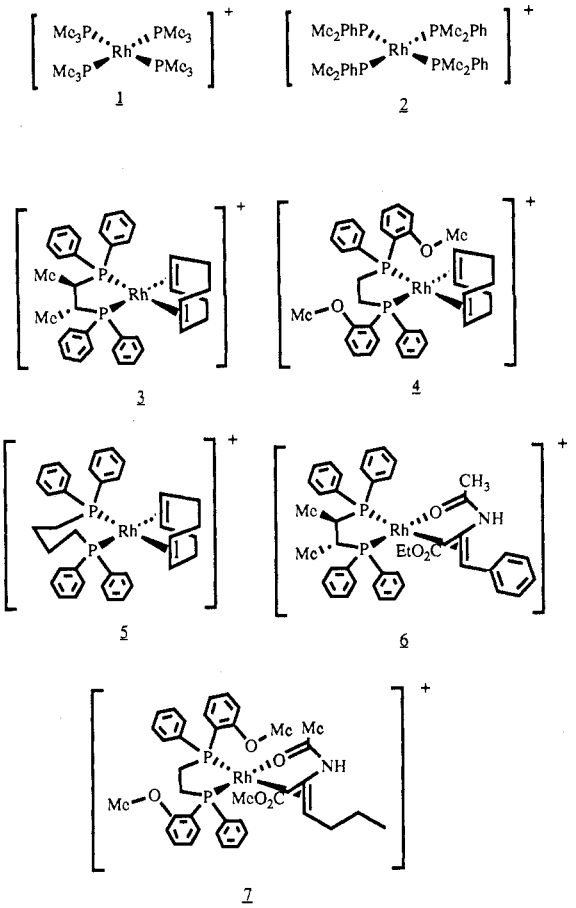

Figure 5. Structures used in the initial parameter development for the SHAPES force field: (**1**) $[Rh(trimethylphosphine)_4]^+$, ref 12; (**2**) [Rh(dimethylphenylphosphine)$_4$]$^+$, ref 49; (**3**) [Rh(*S*,*S*-CHIRAPHOS)(1,5-cyclooctadiene)]$^+$, ref 50; (**4**) [Rh(*R*,*R*-DIPAMP)(1,5-cyclooctadiene)]$^+$, ref 51; (**5**) [Rh(1,4-bis(diphenylphosphino)butane)(1,5-cyclooctadiene)]$^+$, ref 52; (**6**) [Rh(*S*,*S*-CHIRAPHOS)(ethyl (*Z*)α-acetaminocinnamate)]$^+$, ref 53; (**7**) [Rh(*R*,*R*-DIPAMP)(methyl (*Z*)β-propyl-α-acetaminoacrylate)]$^+$, ref 54.

(43) (a) Hay, P. J.; Wadt, W. R. *J. Chem. Phys.* **1985**, *82*, 270. (b) Hay, P. J.; Wadt, W. R. *J. Chem. Phys.* **1985**, *82*, 284. (c) Hay, P. J.; Wadt, W. R. *J. Chem. Phys.* **1985**, *82*, 299.

(44) *MESA: Molecular Electronic Structure Applications*; Saxe, P., Lengsfield, B. H., Martin, R., Page, M.

(45) Gaussian 88: Frisch, M. J.; Head-Gordon, M.; Schlegel, H. B.; Raghavachari, K.; Binkley, J. S.; Gonzalez, C.; Defrees, D. J.; Fox, D. J.; Whiteside, R. A.; Seeger, R.; Melius, C. F.; Baker, J.; Martin, R.; Kahn, L. R.; Stewart, J. J. P.; Fluder, E. M.; Topiol, S.; Pople, J. A. Gaussian Inc., Pittsburgh, PA, 1988.

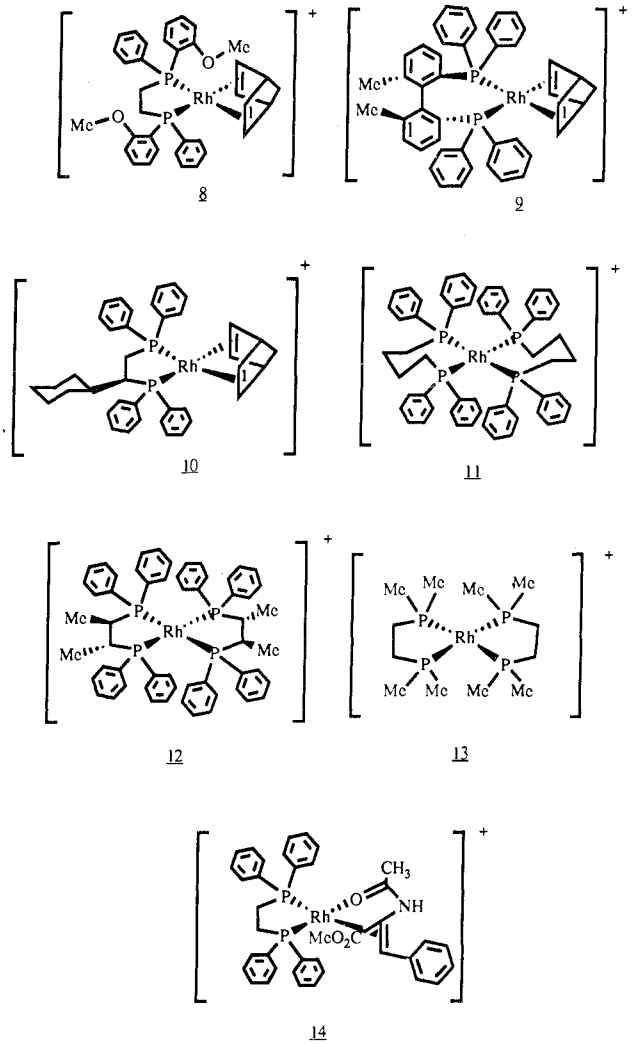

Figure 6. Structures used to test the SHAPES force field parametrization: (**8**) [Rh(*R,R*-DIPAMP)(norbornadiene)]$^+$, ref 55; (**9**) [Rh((+)-(*R*)-2,2′-bis(diphenylphosphino)-6,6′-dimethylbiphenyl)(norbornadiene)]$^+$, ref 56; (**10**) [Rh(CYCPHOS)(norbornadiene)]$^+$, three enantiomorphs, ref 57; (**11**) [Rh(1,4-bis(diphenylphosphino)butane)$_2$]$^+$, ref 58; (**12**) [Rh(*S,S*-CHIRAPHOS)$_2$]$^+$, ref 59; (**13**) [Rh(1,2-bis(dimethylphosphino)ethane)$_2$]$^+$, ref 59; (**14**) [Rh(1,2-bis(diphenylphosphino)ethane)(methyl (*Z*)α-acetaminocinnamate)]$^+$, ref 60.

and angles. The fitting procedure involves iterative adjustment of parameters, followed by energy minimization with the adjusted parameters, followed by comparison of observed and calculated structures. Starting structures are taken from the crystallographic coordinates. A total of 16 crystallographically unique structures were used for this study:[12,46-57] seven structures were selected for the initial parameter development (Figure 5) and the second set of nine structures (Figure 6) was used to test how well the parameters transferred to other complexes.

Table IV. SHAPES Force Field Parameters

bond lengths[b]	r_0, Å	k_r, kcal/(mol·Å^2)	flag[a]
Rh–DETL	2.098	150.0	
Rh–PMET	2.265	90.0	
Rh–PMO	2.206	90.0	
Rh–PMP	2.275	90.0	
Rh–O	2.125	141.0	
PMET–C6R	1.810	232.0	2
PMO–C6R	1.810	232.0	2
PMP–C6R	1.810	232.0	2
PMET–CT	1.824	214.0	3
PMO–CT	1.824	214.0	3
PMP–CT	1.824	214.0	3
bond angles[c]	θ_0, deg	k_θ, kcal/(mol·rad^2)	flag[a]
Rh–PMET–C6R	113.88	40.0	4
Rh–PMO–C6R	116.64	40.0	4
Rh–PMP–C6R	115.29	40.0	4
Rh–PMET–CT	120.50	40.0	5
Rh–PMO–CT	120.50	40.0	5
Rh–PMP–CT	120.50	40.0	5
Rh–O–C	120.00	70.0	
C6R–PMET–C6R	98.67	50.0	6
C6R–PMO–C6R	98.67	50.0	6
C6R–PMP–C6R	98.67	50.0	6
CT–PMP–CT	105.2	50.0	
C6R–PMET–CT	104.9	50.0	7
C6R–PMO–CT	104.9	50.0	7
C6R–PMP–CT	104.9	50.0	7
fourier angle terms[d]	ψ, deg	k^F, kcal/mol	periodicity n	flag[a]
DETL–Rh–DETL	90.00	18.75	2	
	90.00	6.25	4	
PMET–Rh–PMET	90.00	13.12	2	8
	90.00	4.77	4	9
PMP–Rh–PMP	90.00	13.12	2	8
	90.00	5.63	4	
PMO–Rh–PMO	90.00	13.12	2	8
PMET–Rh–DETL	90.00	4.41	4	10
PMO–Rh–DETL	90.00	4.41	4	10
PMET–Rh–PMO	90.00	4.77	4	9
PMO–Rh–DETL	90.00	4.77	4	9
PMET–Rh–O	90.00	5.39	4	11
PMO–Rh–O	90.00	5.39	4	11
DETL–Rh–O	90.00	3.05	4	
O–Rh–O	90.00	7.32	4	

[a] An entry in this column signifies that, during the optimization, all parameters sharing the same flag value were forced to have identical values for the force constants being optimized. [b] Parameters defined according to eq 2 in the text. [c] Parameters defined according to eq 3 in the text. [d] Parameters defined according to eq 6 in the text.

The parameters optimized by the fitting procedure are given in Table IV.[58] Note that some of the parameters are forced to have identical values in the fitting procedure. For example, phosphorus trans to an ethylene (PMET) must be distinguished from phosphorus trans to another phosphorus (PMP) due to the trans influence. Nevertheless, all parameters involving these phosphorus atoms, except the P–Rh bond lengths, were forced to be identical. Not all equilibrium parameters were optimized (e.g. θ_0 for C6R–PMET–C6R) for geometric parameters that were poorly sampled by the parameter development structures. Force constants were optimized for metal bending modes, only, using the SHAPES force field formulation. Recall that SHAPES utilizes 2-fold periodicity for out-of-plane distortions ($E(\theta)$ minima at θ values of 90° and 270°) and 4-fold periodicity for in-plane distortions ($E(\phi)$ minima at ϕ = 0, 90, 180, 270°). Because all of the experimental DETL–RH14–DETL angles are very close to 90°, the angular minimum, optimization of the corresponding force constant was not successful. The value determined from normal coordinate analysis was used instead.

(46) Caulton, K. G. Private communication.
(47) Ball, R. G.; Payne, N. C. *Inorg. Chem.* **1977**, *16*, 1187.
(48) Vineyard, B. D.; Knowles, W. S.; Sabacky, M. J.; Bachman, G. L.; Weinkauff, D. J. *J. Am. Chem. Soc.* **1977**, *99*, 5946.
(49) Anderson, M. P.; Pignolet, L. H. *Inorg. Chem.* **1981**, *20*, 4101.
(50) Halpern, J.; Chan, A. S. C.; Pluth, J. J. *J. Am. Chem. Soc.* **1980**, *102*, 5952.
(51) McCullough, B.; Halpern, J.; Thompson, M. R.; Landis, C. R. *Organometallics*. In press.
(52) Giovannetti, J. S.; Haltiwanger, F. C.; Landis, C. R. Unpublished results.
(53) Svenson, G.; Albertson, J. *Acta Crystallogr.* **1986**, *C42*, 1342.
(54) Oliver, J. D.; Riley, D. P. *Organometallics* **1983**, *2*, 1032.
(55) Young, C. G.; Rettig, S. J.; James, B. R. *Can. J. Chem.* **1986**, *64*, 51.
(56) Marder, T. B.; Williams, I. D. *J. Chem. Soc., Chem. Commun.* **1987**, 1478.
(57) Halpern, J.; Chan, A. S. C.; Pluth, J. J.; Riley, D. P. *J. Am. Chem. Soc.* **1980**, *102*, 5952.

(58) Standard CHARMM Lennard-Jones (LJ) 6–12 parameters were used for all calculations. For phosphorus LJ 6–12 parameters (r_0 = 2.15 Å and ϵ = −0.144 kcal/mol) were determined by least-squares fitting to the Buckingham parameters from MM2. For rhodium the LJ 6–12 parameters used are r_0 = 0.8 Å and ϵ = −0.001 kcal/mol.

Table V. Summary of Experimental and Calculated Averages for All Structures

	Xtal av	calc av (rmsd)[a]	calc av (rmsd)[b]
	Bond Lengths (Å)		
Rh–DETL	2.0950	2.0966 (0.0644)	2.0994 (0.0608)
Rh–PMET	2.2884	2.2809 (0.0256)	2.2836 (0.0271)
Rh–PMO	2.2320	2.2360 (0.0064)	2.2430 (0.0120)
Rh–PMP	2.3016	2.2949 (0.0136)	2.2976 (0.0300)
Rh–O	2.1167	2.1093 (0.0112)	2.1047 (0.0175)
PMET–C6R	1.8089	1.8203 (0.0290)	1.8189 (0.0284)
PMET–CT	1.8356	1.8299 (0.0272)	1.8341 (0.0278)
PMO–C6R	1.8093	1.8207 (0.0447)	1.8193 (0.0448)
PMO–CT	1.8410	1.8283 (0.0243)	1.8347 (0.0206)
PMP–C6R	1.8322	1.8214 (0.0159)	1.8204 (0.0168)
PMP–CT	1.8339	1.8274 (0.0199)	1.8247 (0.0194)
	Bond Angles (deg)		
Rh–PMET–C6R	114.424	114.140 (2.302)	113.686 (2.387)
Rh–PMET–CT	110.194	112.940 (3.016)	113.608 (3.710)
Rh–PMO–C6R	116.430	116.512 (4.755)	116.172 (4.110)
Rh–PMO–CT	110.987	109.690 (1.649)	110.730 (1.250)
Rh–PMP–C6R	115.498	114.121 (4.467)	113.673 (4.469)
Rh–PMP–CT	116.351	116.000 (4.850)	117.974 (5.269)
Rh–O–C	115.033	115.243 (0.949)	113.127 (2.465)
C6R–PMET–C6R	104.804	102.065 (3.474)	101.928 (3.757)
C6R–PMET–CT	105.538	106.327 (3.039)	106.630 (3.166)
C6R–PMO–C6R	105.120	105.773 (1.564)	105.507 (2.132)
C6R–PMO–CT	102.927	103.412 (1.405)	103.365 (0.986)
C6R–PMP–C6R	103.048	103.005 (1.966)	102.376 (1.889)
C6R–PMP–CT	102.046	103.547 (2.035)	103.499 (2.028)
CT–PMP–CT	100.334	102.286 (3.890)	99.162 (3.484)
DETL–Rh–DETL	75.636	81.875 (6.444)	81.833 (6.355)
PMET–Rh–PMET	85.550	82.666 (3.583)	82.240 (3.683)
PMET–Rh–DETL	99.584	97.729 (2.377)	97.964 (2.187)
PMP–Rh–PMP	92.176	91.296 (1.357)	91.079 (2.004)
	161.438	165.258 (6.234)	166.761 (9.252)
PMET–Rh–PMO	83.053	82.970 (0.123)	81.940 (1.146)
PMET–Rh–O	90.407	92.787 (2.867)	92.797 (2.609)
PMO–Rh–DETL	101.230	100.757 (0.497)	101.137 (0.300)
DETL–Rh–O	87.153	83.550 (3.872)	84.103 (3.251)
PMO–Rh–O	170.130	174.053 (5.650)	173.833 (4.147)

[a] Electrostatic interactions were excluded in these calculations. [b] Calculations included electrostatic interactions according to the atom-centered partial charge model.

Note that least-squares fitting of parameters based on a rather small number of test structures will not necessarily give valid results. For example, the "optimized" value for the three types of Rh–P–C6R angles yielded geometries that had Rh–P–C6R angles that were smaller than any of the crystallographic values. After optimization by nonlinear least-squares fitting, all parameters were checked and, if needed, separately adjusted to achieve a better fit to the crystallographic structures. The force field parameters obtained by simultaneous optimization using the nine development structures are listed in Table IV.

IV. Results

In the absence of extensive information concerning the energetics of metal complex conformers, our best test of the quality of the parametrization is a comparison of experimental and computed structures. Next we will (1) examine the overall quality of structures calculated with these parameters, (2) investigate differences between calculation and experiment for a few key structural features, and (3) compare structure-based force constant parameters with those obtained by other means.

1. Computed vs Experimental Structures. In general, the fitting procedure generates parameters capable of simulating the crystallographic structures with impressive accuracy (Table V). For bond lengths, the average root-mean-square deviation (rmsd) is 0.026 Å, and the average rmsd is 3.2° for bond angles. Not surprisingly, the average bond lengths and bond angles are very similar for the experimental and calculated structures (i.e. the fitting procedure works). The largest deviations occur for metal-centered geometric features, most likely reflecting the softer potentials about metals and the strong influence of electronic effects.

Large variations in Rh–P bond lengths occur depending on the nature of the trans ligand. For the complexes used in this study the experimental Rh–P bond lengths ranged from 2.23 to 2.36 Å. The systematic variation of these bond lengths according to the nature of the trans ligand prompted the separation of phosphorus atom types according to the labels PMP, PMO, and PMET. The Rh–P equilibrium bond length parameters increase in the order Rh–PMO (r_0 = 2.206 Å) < Rh–PMET (r_0 = 2.265) < Rh–PMP (r_0 = 2.275) in agreement with the general trend of decreasing bond length with increasing electronegativity of the trans ligand. Identification and analysis of the trans influence (an electronic effect) can be confounded by competing influences on the molecular structure such as the bulk of the ligands (i.e. steric interactions). Empirical force field parameters provide a quantitative, although arbitrary, mechanism for distinguishing steric and electronic effects. Thus, the variation of the Rh–P equilibrium bond length parameters, for which the differing steric requirements of the individual phosphines have been factored out, represents a more definitive observation of the trans influence than averages of crystallographic bond lengths for dissimilar compounds.

The Rh–DETL (rhodium to olefin where DETL is the centroid of the C=C bond) bond lengths are the most difficult bond lengths to simulate. Although the trans ligand is a phosphine for all of the olefin-containing structures examined, the observed Rh–DETL bond lengths vary from 1.91 to 2.16 Å. In fact, the value of 1.919 Å observed for eneamide structure **7** is so far removed from the other values that the validity of the crystallographic result may be questioned. Because all of the structures examined contain chelating olefins, simulation of Rh–DETL bond lengths depends on a balance of ligand-based parameters and metal-centered parameters. Factors that may influence this balance but are not included in our formulation include (1) the "bending back" of the groups attached to the olefin upon coordination to a metal center, (2) shortening of the Rh–DETL bond lengths upon addition of electron-withdrawing groups to the olefin, and (3) variation of the phosphine trans influence with differing trans DETL–Rh–PMET bond angles. For the eneamide complexes, asymmetry in the olefinic C–Rh separations (av C_α–Rh = 2.12 Å, C_β–Rh = 2.16 Å) is observed in the crystal structures but not reproduced by the force field computations. This asymmetry may be influenced more by the presence of strong electron-withdrawing groups on C_α than by the geometrical constraints imposed by chelation of the eneamide.

Bond angles about the metal are described well by the SHAPES force field despite the large range of bond angles observed in the structures tested.[59] For example, the calculated P–Rh–P bond angles (cis angles: 89.1°, 90.1°, 94.7°, 96.1°; trans angles: 150.5°, 160.1°) for the sterically congested complex [Rh(1,4-bis(diphenylphosphino)butane)$_2$]$^+$ (**11**) are just slight underestimations of the observed distortions (cis angles 89.5°, 91.0°, 95.9°, 96.1°; trans angles 150.5°, 155.6°) from idealized square-planar geometries (cis angles 90°; trans angles 180°). A superposition of the calculated and experimental structures for **11** is shown in Figure 7. The slight underestimations of angular distortions are a general feature of the current SHAPES parameters for square-planar complexes, suggesting that slightly smaller angular force constants (for the θ term in particular) may be required.

Metal-centered bond angles involving olefinic ligands are more difficult to fit. In our test structures the norbornadiene ligand presents the greatest challenge due to the requirement of balancing strain about the bridgehead position with the strain induced by the small bite angle of the diene. For example, the coordinated norbornadiene ligand of the complex [Rh(DIPAMP)(norbornadiene)]$^+$ (**8**) contains a highly strained (experimental C(vinyl)–C(bridgehead)–C(vinyl) = 95.4°) bond angle about the sp^3-hybridized bridgehead carbon. Treatment of the bridgehead carbon with the normal CHARMM harmonic term and the

(59) For test structure **9**, standard CHARMM parameters were used for torsions about the Ph–Ph bond of the biphenyl group. These torsions are too stiff resulting in a corresponding torsion angle of −44° compared with an experimental value of −71°. However, the bond lengths and angles about the metal center were not adversely affected.

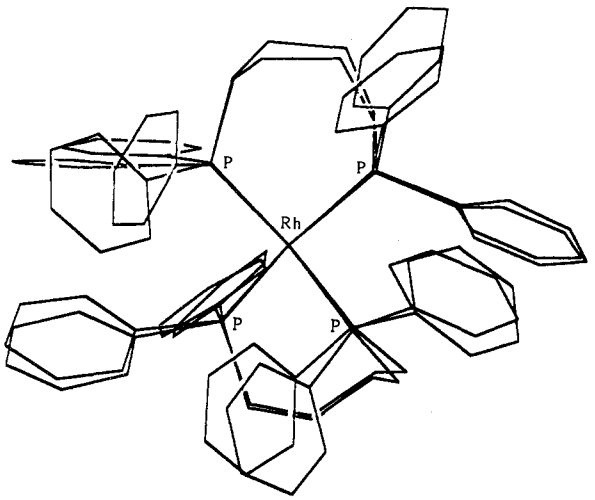

Figure 7. The superposition of the crystallographic and the SHAPES energy minimized structures for $[Rh(1,4\text{-bis(diphenylphosphino)butane})_2]^+$ (**11**). The perspective is from above the coordination plane.

standard CHARMM parameters yields a 101.8° bond angle value whereas a 97.0° value is obtained with use of the softer Fourier term for the bridgehead angles. For all structures containing the coordinated norbornadiene ligand, the bite angle (DETL–Rh–DETL) is calculated to be larger than the observed value. On average this discrepancy is about 7°. Presumably, this discrepancy reflects the delicacy with which the distortion potentials for the metal-centered angle and the bridgehead-centered angle must be balanced. The chelating diolefin, 1,5-cyclooctadiene, has a bite angle close to 90° in the structures examined and, hence, the calculated bite angles are not very sensitive to the parametrization.

Our principal interest in parametrizing square-planar complexes of rhodium is the investigation of structural origins of selectivity in catalytic processes. The eneamide complexes **6**, **7**, and **14**, which are intermediates in asymmetric hydrogenation reactions, have structures that are modeled well by the SHAPES force field. For example, the average O–Rh–P angles are calculated to be 92.7° (cis) and 173.8° (trans) compared with the crystallographic averages of 90.5° and 170.1°, respectively. The DETL–Rh–P averages do not agree as well: the calculated averages are 101.2° (cis) and 176° (trans) and the crystallographic averages are 100.9° (cis) and 160.9° (trans). The trans DETL–Rh–P angle discrepancy is large and can be traced by two factors. The first factor is an overestimation of the angular distortion force constant which was mentioned previously. In particular, the out-of-plane distortion potentials appear to be too steep, resulting in underestimation of the distortion from planarity and, hence, trans bond angles that are closer to 180° than is observed. The second factor is the location of the point of metal-to-olefin attachment along the C=C axis. Our current version of the program calculates this point as equidistant between the two carbon atoms, whereas intuition, based on binding constant and structural trends concerning metal–olefin bonds,[60] suggests that this point should favor the carbon with more electron withdrawing groups attached. Adjustment of the metal–olefin attachment point toward the α-carbon would shorten the Rh to α-carbon distance relative to the Rh to β-carbon distance and decrease the trans DETL–Rh–P angle values.

2. Structure-Based Parameters. Values of the P–Rh–P bond angles vary significantly from equilibrium values (90° and 180°) in the structures examined (cis angle deviations up to 10° and trans angle deviations as large as 32°). This variability suggests that force constants for bending these angles may be approximated from structural data. Our fitting procedure yields harmonic force constants of 26 and 38 kcal/(mol·rad^2) for out-of-plane and in-plane distortions, respectively, which compare well with the ab initio values of 20 and 43 kcal/(mol·rad^2), respectively. Of course the uncertainties in these values are rather large (ca. ±30%) and definitive conclusions cannot be drawn from such a limited data set. It is reassuring, however, to obtain compatible values from completely different methods. As the determination of these force constants from vibrational data is undermined by experimental problems, it would appear that structure-based methods and ab initio methods may be the only practical alternatives.

3. Inclusion of Electrostatic Interactions. The work described to this point reflects parameter development in the absence of electrostatic interactions. Electrostatic interactions have been claimed to exert little effect on structures but to exert considerable influence on molecular energetics.[61] We have examined the influence of electrostatics on molecular structure using atom-centered charges calculated by the charge equilibration method developed by Rappe and Goddard.[62] This method predicts charge distributions in molecules for use in molecular dynamics simulations based on the equalization of chemical potentials. Partial charge distributions calculated in this way have the important feature of being dependent on the molecular geometry.

Currently we use the calculated charges without further verification. For the sixteen structures analyzed, the average atomic partial charges are as follows: Rh14 (+0.43), PMP (−0.11), PMET (−0.10), PMO (−0.07), ETRH (−0.06), and O (−0.62). We are in the process of comparing these charge distributions with those determined from ab initio electrostatic potential calculations.

All structures were energy minimized using the developed parameters but with the inclusion of charges; parameters were not reoptimized with charges. The calculated average structural values and their rmsd from the crystallographic values in Table V indicate that the structures are not significantly influenced by the inclusion of electrostatic interactions. This result suggests that parameters developed without partial charges can be transferred to charged complexes.

V. Discussion

1. SHAPES Formulation. The SHAPES formulation of angular potentials in empirical force fields provides a flexible and convenient description of complex molecular geometries, such as those observed for many common transition-metal complexes. Expression of angular terms as a Fourier expansion (truncated at one term) is supported for the simple example of water by angular overlap arguments and by comparison of ab initio results with empirical force field calculations. The SHAPES formulation is not derived directly from angular overlap considerations, rather, it is an intuitive development of internal coordinates and potential functions. In fact, the general idea of angular potentials reflecting the loss of angular overlap is not original with us. In the orbital valence force field proposed by Linnett and Heath[63] in 1948 "it is assumed that the bond-forming orbitals of an atom X are set at definite angles to each other, and that the most stable bond is produced when one of these orbitals overlaps the bond-forming orbital of the second atom Y to the maximum possible extent". Incorporation of spherical internal coordinates provides a convenient method of describing angle deformations and replaces the more common improper dihedral and bond angle internal coordinates. The combination of the spherical internal coordinates with periodic Fourier potential expression permits the symmetry of idealized molecular shapes to be accommodated simply. As a result, redundant atom-labeling schemes are not required to distinguish cis vs trans ligand arrangements and complex geometries, such as the trigonal bipyramid, are described efficiently. In addition, the resulting angular potential energy surfaces are smooth and without cusps at all geometries.

The Fourier angular potential parameters are readily derived from harmonic parameters by using simple expressions. The

(60) Tolman, C. A. *Chem. Rev.* **1977**, *77*, 313.

(61) Pettit, B. M.; Karplus, M. *J. Am. Chem. Soc.* **1985**, *107*, 1166.
(62) Rappe, A. K.; Goddard, W. A. *J. Chem. Phys.* In press.
(63) Heath, D. F.; Linnett, J. W. *Trans. Faraday Soc.* **1948**, *44*, 873.
(64) (a) Burdett, J. K. *Molecular Shapes*; Wiley-Interscience: New York, 1980: Chapters 2, 6, and 9. (b) Larsen, E.; La Mar, G. N. *J. Chem. Ed.* **1974**, *51*, 633.
(65) Goddard, W. A.; Harding, L. B. *Annu. Rev. Phys. Chem.* **1978**, *29*, 363.

Fourier potentials are identical with harmonic potentials for small displacements from the equilibrium position but are "softer" for large displacements. This feature effects lower (more realistic?) angular strain energies for Fourier terms than for harmonic terms in computations involving large displacements from equilibrium (e.g. cyclopropane). The accuracy of computations on metal complexes, which often exhibit large deviations of bond angles from equilibrium, also should benefit from softer potentials.

SHAPES is not necessarily the preferred force field formulation for all molecules. For organic molecules (sp, sp^2, and sp^3 hybridization) the usual internal coordinates and harmonic or, more preferred, Fourier expressions work well and require a minimum of parameters. Because SHAPES expressions are based on idealized geometries, the equilibrium positions are fixed and are more difficult to adapt to non-idealized equilibrium geometries. However, alternative geometries can be accommodated by expansion of the Fourier terms. Also, the SHAPES formulation has an inherent problem: the presence of minima at 0° angles (ϕ or θ). This problem points out the need for some form of 1,3 interaction. It is frequently assumed that 1,3 interactions are implicitly included in the angle-bending potential, regardless of whether the potential is harmonic or Fourier. The HF–SCF calculations for water show that this assumption is not valid for small bond angles (or small interligand separations) and demonstrate the need for 1,3 interactions for valence force fields as well as for the SHAPES force field.

2. Parametrization of Metal Complexes. Metal complexes present difficulties in developing parameters because of the presence of large electronic influences and because of the low frequencies of the metal–ligand vibrational modes. We have presented three approaches to determining force constants for metal–ligand vibrations. Normal coordinate analysis with a simple valence force field may be applied to a limited number of transition-metal complexes. Although the observed bands can be reproduced with acceptable accuracy, there are large uncertainties in some of the force constants. Bending mode force constants are not well determined due to the difficulty of assigning these modes. Force constants for M–P stretching modes are poorly determined due to extensive mixing of C–P–C bending modes with the M–P stretches. However, normal coordinate analysis does yield useful force constants for M–halogen, M–ethylene, and M–ammine stretches which can be used to calibrate our other approaches.

A second approach uses HF–SCF calculations to estimate force constants. Although the computed bond lengths for metals bound to third row atoms are longer by ca. 0.1 Å than those found experimentally, the computed stretching force constants are in good agreement with those determined by normal coordinate analysis. Ab initio calculations have the advantage, in principle, of being applicable to any model compound. Practical limitations are imposed by the computational time required (these limitations are mitigated to a large extent by the use of effective core potential basis sets), the cumbersome and inexact method of second derivative estimation employed, and uncertainties concerning the accuracy of the results. On the basis of a limited number of test cases, the computed force constants appear to agree with empirical values within the limits of experimental uncertainty.

Structure-based force constant parametrization makes productive use of the problem of large variations in metal complex geometries. Angular displacements are frequently large and are sensitive to the value of the force constants. For these cases, optimization of the force constants according to the best fit between crystallographic and computed structures is successful and gives values similar to those calculated by other methods. However, the method is not successful when large variations from the equilibrium are not observed, such as for bond lengths.

3. Future Directions. The development of the SHAPES force field and the approaches to force field parametrization outlined in this paper illustrate some of the problems associated with the application of empirical force field calculations to transition-metal complexes and suggest some ways to mitigate these problems. Future efforts will be aimed at (1) developing generic (albeit crude) parameters for metals differing in formal oxidation states and in idealized geometries, (2) molecular dynamics investigations of the origins of selectivity in homogeneous catalysis, with an emphasis on catalytic, asymmetric hydrogenation, and (3) further improvements in the SHAPES force field, including a more general treatment of the trans influence, addition of 1,3-interaction terms, and the inclusion of analytical second derivatives for the SHAPES terms.

Appendix 1

First, we consider the two-dimensional molecule water. According to the AOM,[64] the angular potential energy surface is determined by the balance of stabilizing quadratic terms (e_σ) and destabilizing quartic terms (f_σ) arising from the overlap of oxygen 2p orbitals and the hydrogen 1s orbitals (eqs 15 and 16)

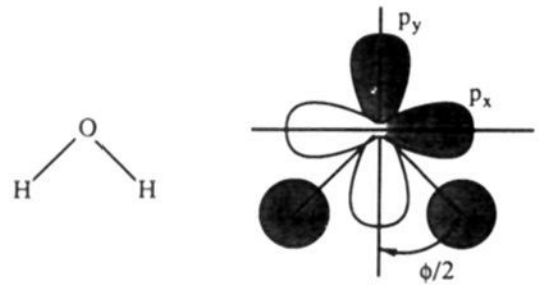

$$E_{AOM} = E_{p_x} + E_{p_y} \tag{14}$$

(where E_{p_x} and E_{p_y} refer to the energies of the filled molecular orbitals derived from overlap of the $2p_x$ (or a_1) and $2p_y$ (or b_2) oxygen atomic orbitals with the hydrogens)

$$E_{AOM} = 4e_\sigma[\sin^2(\phi/2) + \cos^2(\phi/2)] - 8f_\sigma[\sin^4(\phi/2) + \cos^4(\phi/2)] \tag{15}$$

$$E_{AOM} = 4e_\sigma - 8f_\sigma[\sin^4(\phi/2) + \cos^4(\phi/2)] \tag{16}$$

Using this p orbital only model, the stabilizing e_σ terms are angle independent (being proportional to the sum, $\sin^2(\phi/2) + \cos^2(\phi/2)$) leaving the determination of the molecular geometry to minimization of the destabilizing f_σ terms (eq 15). For water, orbital destabilizations are minimized at a bond angle of 90° ($\phi/2 = 45°$) leading to the prediction of a bent shape for water and an energy maximum at the linear geometry. One method of casting this result into a form commensurate with the potential energy formalism of EFF computations utilizes a single 2-fold (i.e. $n = 2$) Fourier term in the bond angle ϕ (eq 6). In fact, by using standard trigonometric relationships the Fourier term exactly simulates the AOM function when the molecular energies are expressed according to the potential energy formalism of EFF calculations (eqs 17–20).

$$E_{AOM} = 4e_\sigma - 6f_\sigma - 2f_\sigma \cos(2\phi) \tag{17}$$

$$E_{AOM}^{strain} = E_{AOM} - E_{AOM}^{min} \tag{18}$$

$$E_{AOM}^{strain} = -2f_\sigma[1 + \cos(2\phi)] \tag{19}$$

$$E_{EFF} = E_{AOM}^{strain} \text{ when } \psi = 0 \text{ and } k^F = -2f_\sigma \tag{20}$$

Note that Fourier terms for angular deformations, unlike harmonic potentials, are periodic and reach a maximum at the linear geometry. Therefore, Fourier terms (and the related cosine expansions) are better behaved functions for angular distortion potentials than the harmonic terms. Using the relationship, $\phi \cong \sin\phi$ at small values of ϕ, the harmonic force constant (eq 3), k^H, is simply related to the Fourier "force constant", k^F, for a Fourier term with periodicity, n (eq 9). This relationship provides a convenient expression for interconversion of force constants.

Of course, water does not have a 90° bond angle. (However, electronic structure calculations[65] do suggest that ligand-central atom overlaps favor ~90° bond angles, as found in H_2S; Pauli bond repulsions are responsible for opening of the angle when the central atom–ligand distances are short, as in water.) The Fourier term readily accommodates the experimental geometry for water ($\phi = 104°$) by adjustments of the "force constant", k^F, the periodicity, and the phase angle, ψ. For a bond angle with the equilibrium position ϕ_0 and harmonic force constant k, the Fourier

terms (n, k^F, and ψ) adapted to give a maximum in $E(\phi)$ at $\phi = 180°$ are given by eqs 7-9.

Appendix 2

The SHAPES force field is the three-dimensional generalization of the Fourier angular potential expressions. In order to illustrate the SHAPES formulation and its relationship to the AOM we will first consider angular distortions for ammonia according to the AOM.[15] For this discussion the geometric arrangement and angle definitions illustrated in Figure 2 are adopted. Two distortion coordinates, θ (the angle formed by the z axis and the N-H bond vector, or the inversion coordinate) and ϕ (the angle formed by the projections of the N-H bond vectors into the x-y plane), are considered with the simplifying constraints that $\theta_1 = \theta_2 = \theta_3$ and $\phi_{12} = \phi_{23} = \phi_{13}$. According to the p-orbital AOM (i.e. utilizing the 2p orbitals, only, of the nitrogen) the total energy is given by

$$E_{AOM} = 4e_\sigma[(1 + 2\cos^2\phi)(\sin^2\theta) + 2\sin^2\phi\sin^2\theta + 3\cos^2\theta] - 4f_\sigma[(1 + 2\cos^2\phi)^2(\sin^4\theta) + 4\sin^4\theta\sin^4\phi + 9\cos^4\theta] \quad (17a)$$

$$E^{strain}_{AOM} = 12f_\sigma - 4f_\sigma\{[5 + (4\cos^2\phi)(2\cos^2\phi - 1)][\sin^4\theta] + 9\cos^4\theta\} \quad (17b)$$

These expressions lead to a total of four minima symmetrically disposed about $\phi = 90°$ and $\theta = 90°$. Two of these minima ($\phi = 120°$ and $\theta = 54.7°$ and 125.3°) closely correspond to the experimental structure of NH_3 ($\phi = 120°$ and $\theta \cong 59°$ and 121°) whereas the two minima at $\phi = 60°$ and $\theta = 54.7°$ and 125.3° are not observed. The second set of minimum energy structures occurs because the AOM does not take into account interligand overlaps (1,3-interactions). Note that the ϕ terms of expression 17b are multiplied by $\sin^4\theta$, reflecting decreasing overlap of the p_x and p_y orbitals of the central nitrogen with the ligands as the ligands are displaced from the x-y plane. These changes give rise to the weighting formula used in SHAPES (eq 11), where $\sin\theta \approx r_{ML}/R_{ML}$.

Acknowledgment. Partial support of this work by the donors of the Petroleum Research Fund, administered by the American Chemical Society, is gratefully acknowledged. We thank the Monsanto Company and Syntex Corp. for additional support. Polygen Corp. supplied us with the source code for the CHARMM program for which we are most thankful. We thank A. K. Rappe for providing us with the computer code for the calculation of partial charges by the charge equilibration method and for many helpful discussions. Finally, we acknowledge P. J. Hay for his assistance in using the MESA computational package and for his encouragement and advice.

Registry No. 8, 75085-37-9; **9**, 91514-09-9; **10**, 75421-75-9; **11**, 70196-22-4; **12**, 97860-28-1; **13**, 60362-57-4; **14**, 70376-39-5; *trans*-$Pd(NH_3)_2Cl_2$, 13782-33-7; *trans*-$Pt(NH_3)_2Cl_2$, 14913-33-8; $[Rh(PH_3)_4]^+$, 121176-09-8; $[PdCl_4]^{2-}$, 14349-67-8; $[Pt(NH_3)_4]^{2+}$, 16455-68-8; $[Pd(NH_3)_4]^{2+}$, 15974-14-8; $[Pd(PMe_3)Cl_3]^-$, 44630-56-0; $[Pt(PMe_3)Cl_3]^-$, 44630-63-9; *trans*-$^{104}Pd(PEt_3)_2Cl_2$, 29303-43-3; *trans*-$^{110}Pd(PEt_3)_2Cl_2$, 130434-99-0; $[Pt(C_2H_4)Cl_3]^-$, 12275-00-2; $[Pt(C_2D_4)Cl_3]^-$, 69030-45-1; $[Rh(C_2H_4)_2Cl]_2$, 12081-16-2; *trans*-$Rh(PMe_3)_2(CO)Cl$, 22710-50-5; *trans*-$Pt(PH_3)_2Cl_2$, 79389-91-6; *trans*-$Pd(PH_3)_2Cl_2$, 72360-10-2; $[PtCl_4]^{2-}$, 13965-91-8.

Supplementary Material Available: Tables of the results of normal coordinate analyses of $[PtCl_4]^{2-}$, $[PdCl_4]^{2-}$, $[Pt(NH_3)_4]^{2+}$, $[Pd(NH_3)_4]^{2+}$, *trans*-$Pt(NH_3)_2Cl_2$, *trans*-$Pd(NH_3)_2Cl_2$, $[Pd(PMe_3)Cl_3]^-$, $[Pt(PMe_3)Cl_3]^-$, *trans*-$^{104}Pd(PEt_3)_2Cl_2$ and *trans*-$^{110}Pd(PEt_3)_2Cl_2$, $[Pt(C_2H_4)Cl_3]^-$ and $[Pt(C_2D_4)Cl_3]^-$, $[Rh(C_2H_4)_2Cl]_2$, and *trans*-$Rh(PMe_3)_2(CO)Cl$, the HF-SCF optimized geometries for *trans*-$Pt(NH_3)Cl_2$, *trans*-$Pt(PH_3)_2Cl_2$, *trans*-$Pd(NH_3)_2Cl_2$, *trans*-$Pd(PH_3)_2Cl_2$, and $[Rh(PH_3)_4]^+$, and tabulation of SHAPES calculated and experimental structures for compounds **1-14** (51 pages). Ordering information is given on any current masthead page.

Formation of Self-Assembled Monolayers by Chemisorption of Derivatives of Oligo(ethylene glycol) of Structure $HS(CH_2)_{11}(OCH_2CH_2)_mOH$ on Gold[1]

Catherine Pale-Grosdemange, Ethan S. Simon, Kevin L. Prime,[†] and George M. Whitesides*

Contribution from the Department of Chemistry, Harvard University, Cambridge, Massachusetts 02138. *Received May 21, 1990*

Abstract: This paper describes the preparation of oligo(ethylene glycol)-terminated alkanethiols having structure $HS(CH_2)_{11}(OCH_2CH_2)_mOH$ ($m = 3$-7) and their use in the formation of self-assembled monolayers (SAMs) on gold. A combination of experimental evidence derived from X-ray photoelectron spectroscopy (XPS), measurement of contact angles, and ellipsometry implies substantial disorder in the oligo(ethylene glycol)-containing segment. The order in the $-(CH_2)_{11}-$ group is not defined by the available evidence. The SAMs are moderately hydrophilic: $\theta_a(H_2O) = 34$-38°; $\theta_r(H_2O) = 22$-25°. A study of monolayers containing mixtures of $HS(CH_2)_{11}CH_3$ and $HS(CH_2)_{11}(OCH_2CH_2)_6OH$ suggests that the oligo(ethylene glycol) moieties are effective at preventing underlying methylene groups from influencing wetting by water. A limited study demonstrates that these oligo(ethylene glycol)-containing SAMs resist the adsorption of protein from solution and suggests that SAMs will be a useful model system for studying the adsorption of proteins onto organic surfaces.

Introduction

Oligomers of ethylene glycol are moderately hydrophilic groups: The Hansch π parameter for ethylene glycol is $\sim$-1.93.[2] These oligomers are commonly incorporated as components of materials when increased hydrophilicity is required[3] and have proved useful as constituents of biocompatible materials.[4] The structure of the oligo(ethylene glycol) units at a solid-water interface is relevant to the molecular level design of materials having desired degrees

[†] NSF Predoctoral Fellow, 1986-1989.

(1) The research described in this paper was supported by the National Science Foundation under the Engineering Research Center Initiative to the MIT Biotechnology Process Engineering Center (Cooperative Agreement CDR-88-03014), by the Office of Naval Research and the Defense Advanced Research Projects Agency, and by the NIH (GM39589). The XPS was provided by DARPA through the University Research Initiative and is housed in the Harvard University Materials Research Laboratory, an NSF-funded facility.

0002-7863/91/1513-12$02.50/0